

The oxidative dehydrogenation of propane over potassium-promoted molybdenum oxide/sol–gel zirconia catalysts

S.N. Koc^{a,*}, G. Gurdag^a, S. Geissler^b, M. Guraya^{b,1}, M. Orbay², M. Muhler^b

^a Department of Chemical Engineering, Faculty of Engineering, Istanbul University, 34320 Avcilar, Istanbul, Turkey

^b Laboratory of Industrial Chemistry, Faculty of Chemistry, Ruhr-University Bochum, D 44780 Bochum, Germany

Received 7 July 2004; received in revised form 3 September 2004; accepted 4 September 2004

Available online 12 October 2004

Abstract

The effect of potassium loading on the structural and catalytic properties of MoO_x/ZrO₂ catalysts for oxidative dehydrogenation of propane was investigated. Catalysts have been prepared by modified sol–gel method, and they were characterized by nitrogen physisorption, XRD, FT-Raman spectroscopy, XPS and temperature-programmed reduction (TPR). Catalytic activity measurements have been carried out between 400 and 530 °C under atmospheric pressure. It was observed that potassium addition prevented crystalline Zr(MoO₄)₂ formation, suppressing the interaction of molybdenum oxide and zirconia phases, and it also favored the formation of three-dimensional molybdenum oxide and two-dimensional polymolybdates. Both propylene selectivity and yield were enhanced with a certain amount of potassium addition.

© 2004 Elsevier B.V. All rights reserved.

Keywords: Oxidative dehydrogenation; Molybdenum oxide; Zirconia; Sol–gel; Alkali promotion

1. Introduction

Conversion of lower alkanes by oxidative transformation to corresponding alkenes has gained importance in recent years [1,2]. Nowadays, propylene is produced by cracking of naphtha and gas oil, and by non-oxidative conversion of propane. On the other hand, the oxidative dehydrogenation (ODH) of propane provides an additional alternative production route for propylene. Furthermore, oxidative dehydrogenation reaction is quite exothermic and the energy requirement can be partially met by the combustion of abstracted hydrogen atoms. In addition, neither coking nor frequent regeneration problems occur. From thermodynamic point of view, up to 100% conversion is possible. However, allylic C–H bond of propylene is weaker than the secondary C–H

bond of propane [3], and propylene selectivity is the main problem at high propane conversion levels. This in turn causes a handicap for acidic catalytic surfaces necessary for propane activation, because propylene desorption from surface is not fast enough and even worse it is adsorbed on other sites. In both cases it burns to CO_x while the initial selectivity of propylene is high [4]. Thus, studies on ODH of propane are concentrated on activation mechanism of propane, effect of oxygen type on product selectivity, and the effect of either reaction conditions or catalyst composition on the reaction mechanism [1].

A significant amount of work was carried out for the ODH of propane over molybdenum oxides and metal molybdates [4–11]. For example, Stern and Graselli [9] have determined that among the metal molybdates, nickel molybdate showed the highest ODH performance. An increase in the catalytic activity in the presence of MoO₃ was observed by Cadus et al. [7], Lezla et al. [8] and Miller et al. [12] for MgMoO₄ catalysts. But, they also mentioned that if the content of excess MoO₃ units on the surface is higher than a specific amount, activity decreases probably due to forma-

* Corresponding author. Tel.: +90 212 5912479; fax: +90 212 4737038.

E-mail address: nacik@istanbul.edu.tr (S.N. Koc).

¹ On leave from Centro Atomico Bariloche 8400-S.C. de Bariloche, Argentina.

² Retired from Chemical Engineering Department of Istanbul University.

tion of $\text{Mg}_2\text{Mo}_3\text{O}_{11}$ by the solid-state reactions. Meunier et al. [10] worked with molybdenum oxide-type catalysts with alumina, zirconia and titania supports. They found out that what type of MoO_x species is going to form is determined by the surface molybdenum density as well as the interaction between active component and support. These properties also affect the product selectivity on the ODH of propane [11,13]. Duhamel et al. [14] worked with $\text{MoO}_3/\text{Al}_2\text{O}_3$ catalysts and reported that hydroxyl groups on the surface of catalysts acted as hydrogen acceptors inhibiting CO_x formation. Chen et al. [15] reported that alkali addition to $\text{MoO}_x/\text{ZrO}_2$ catalysts reduced the turnover number, but increased the propylene selectivity. On the other hand, Watson and Ozkan [16] reported that alkali addition up to a certain level increased both propane conversion and propylene selectivity over $\text{MoO}_3/\text{TiO}_2\text{-SiO}_2$ catalysts prepared by sol-gel co-precipitation method.

Sol-gel method has been frequently employed for high-purity catalyst preparation during the last decade [17]. Some properties such as surface area, pore structure, distribution of active sites, and thermal stability which are the main parameters affecting the catalytic activity, can be controlled. These properties depend on several parameters such as the type of raw materials, solvents, acid/base ratio, amount of water, aging and drying, and calcination conditions [18].

In this work, we aimed to investigate the use of alkali-promoted $\text{MoO}_x/\text{ZrO}_2$ catalysts prepared by sol-gel method in ODH of propane. The effect of alkali addition on the structure of supporting oxide, the type of MoO_x units and their effect on the propylene yield and selectivity were investigated.

2. Experimental

2.1. Catalyst preparation

Catalysts with 11.5% (wt) MoO_3 content were prepared by sol-gel method. Zirconium (IV) propoxide (70% solution in propanol, Fluka), ethylacetoacetate (Merck), *i*-propanol (Merck), ammonium heptamolybdate (Merck), 25% aqueous ammonia solution (Carlo Erba), and KOH (Merck) were used as starting materials. In the first step of catalyst preparation, zirconium (IV) propoxide was added to *i*-propanol and ethylacetoacetate mixture under vigorous stirring to provide final alkoxide to solvent and ligand agent ratios of 1:3 and 1:2, respectively. Afterwards, ammonia solution, 0.5 M KOH, 0.25 M ammonium heptamolybdate solution and water were added dropwise for 30 min; the molar ratios of water and ammonia to alkoxide were 7:1 and 5:1, respectively. All gels were dried at 120 °C for 8 h and calcined in air at 540 °C for 3 h. K was added according to K/Mo molar ratios of 0, 0.05, 0.15, 0.25, 0.50, and the amount of K in the catalysts was indicated as K0 (K-free), K005, K015, K025, and K050 in tables and figures.

2.2. Catalysts characterization

Nitrogen physisorption measurements were carried out at -196°C with 150 mg samples by Quantachrome Autosorb 1C after high-vacuum degassing of the catalysts at 300 °C. XRD patterns were obtained from Siemens D type diffractometer by using Cu $K\alpha$ irradiation ($\lambda = 1.5404 \text{ \AA}$). Raman spectra were recorded using Nicolet Nexus FT-Raman Spectrometer equipped with an InGaAs detector. Raman scattering was excited with a Nd-YAG laser operated between 150 and 1200 cm^{-1} region with 4 cm^{-1} resolution under dehydrated conditions. XP spectroscopy measurements were performed in an ultra high vacuum set-up equipped with a Gamdata-Scienta SES 2002 analyzer with various entrance slits. Monochromatised Al $K\alpha$ (1486.6 eV; 14 kV; 55 mA) was used as incident radiation. XP spectra were recorded in fixed transmission mode. The energy resolution was determined as 0.5 and 1.5 eV, respectively. Zr $3d_{5/2}$ structure was used as internal standard at 182.2 eV of binding energy. Temperature-programmed reduction (TPR) experiments were carried out with 150 mg samples of 250–355 μm size placed in a quartz micro reactor under atmospheric pressure. Reactor was heated up to 850 °C at a rate of 10 °C/min under H_2/Ar flow of 50 mL/min with a content of 4.7% H_2 . Water was eliminated in a cold trap and hydrogen was determined by an on-line Hydros 100 TCD system.

2.3. Catalytic measurements

The ODH reaction of propane was carried out with a fixed-bed U-type quartz reactor. Propane (99.95%, Linde), oxygen (99.99%, Messer-Griesheim) and neon (99.99%, Messer-Griesheim) were fed at atmospheric pressure with the composition of 8:8:59, respectively, to provide a total flow rate of 75 ml/min. Uniform temperature distribution was provided by a furnace with fluidized bed sand bath. Catalysts of 250–355 μm size were diluted with quartz chips at a weight ratio of 1:1 to provide a 2 g catalysts charge. The dead volume of the reactor was filled with quartz chips in order to avoid homogenous reactions. Satochrome on-line GC system with TCD and FID detectors, molecular sieve 5A column for Ne, O_2 and CO, and PoraPLOT Q column for hydrocarbons, CO_2 and H_2O were used for the analysis.

3. Results

3.1. Catalysts characterization

Nitrogen physisorption data of molybdenum oxide catalysts are given in Table 1. Although alkali addition had no significant effect on the surface areas, pore volume/diameter values showed distinct maximum for K015.

The diffractograms of K0 and K050, which show maximum difference, are given in Fig. 1. In the case of K050 catalyst, the most intense peak indicating the formation of

Table 1
Nitrogen physisorption results of K-MoO_x/ZrO₂ catalysts

Catalyst	Surface area (m ² /g)	Pore volume V _g (cm ³ /g)	Mean pore diameter (Å)
K0	89	0.043	19
K005	86	0.069	32
K015	101	0.112	44
K025	91	0.084	37
K050	82	0.083	41

tetragonal zirconia was observed at $2\theta = 31.1$ (JCPDS/24-1164), but no peak due to monoclinic phase was detected. Tetragonal zirconia converts into monoclinic phase nearly at 450 °C under suitable conditions, but as previously reported [19], the presence of MoO_x units in the catalyst structure stabilizes the tetragonal phase and prevents its transformation to the monoclinic form. On the other hand, in the case of K-free catalyst (K0), an additional Zr(MoO₄)₂ phase was detected by the peak at $2\theta = 24.0$ (JCPDS/21-1469), and no peak attributed to crystalline MoO₃ peak was observed. The absence of crystalline MoO₃ peak probably indicates that MoO_x units are either highly dispersed or amorphous in nature [13]. In the diffractogram of K050 catalyst, the Zr(MoO₄)₂ peak disappeared with potassium addition, and the tetragonal zirconia peak became sharper and no peak due to potassium molybdate phase was observed.

The Raman spectra of the catalysts with different K contents are given in Fig. 2. The peaks with low intensity at 270, 312, 456 and 648 cm⁻¹ are ascribed to tetragonal zirconia phase [20–22], and K addition increases the peak intensities. Monoclinic phase of zirconia was not observed, which is usually identified by a prominent peak at 490 cm⁻¹ [23]. Peaks at 745 and 948 cm⁻¹ are due to Zr(MoO₄)₂ phase [22,24] and their intensities decrease with K loading, and finally disappear above 15% K. This is in accordance with X-ray diffractograms. Peaks at 819 cm⁻¹ indicate Mo–O–Mo stretching of three-dimensional molybdenum oxide domains [13,22,25], and its intensity was obviously increased by potassium loading. Peak at 972 cm⁻¹ attributed to the stretching of Mo=O bonds. Despite being barely observable for K-free catalyst, it appears and increases

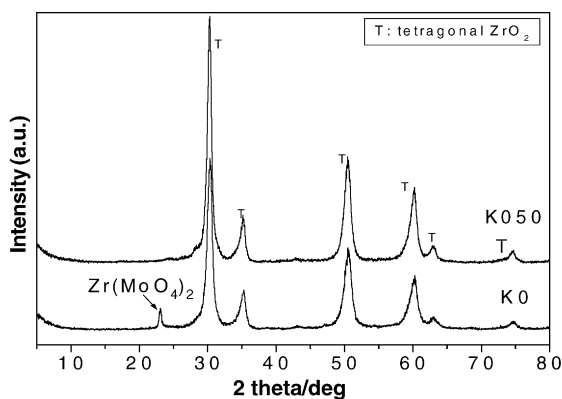


Fig. 1. XRD patterns of K0 and K050 catalysts.

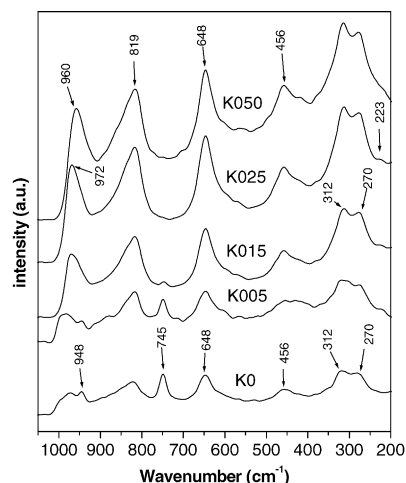


Fig. 2. Raman spectra of K-MoO_x/ZrO₂ catalysts.

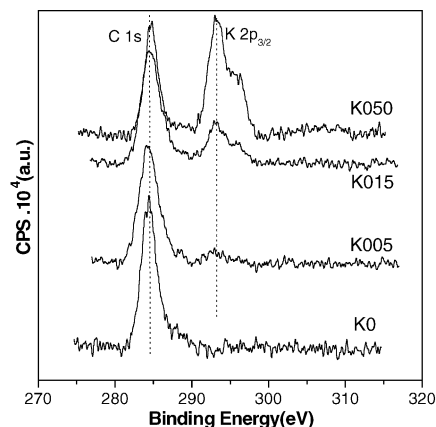


Fig. 3. K 2p_{3/2} XP spectra of catalysts.

in intensity as the amount of K increases indicating the formation of two-dimensional polymolybdates [13,22].

The K 2p_{3/2}, C 1s and Mo 3d_{5/2} XP spectra are shown in Figs. 3 and 4, respectively. The K 2p_{3/2} intensity at 293.2 eV increases gradually with K loading. The XPS results are

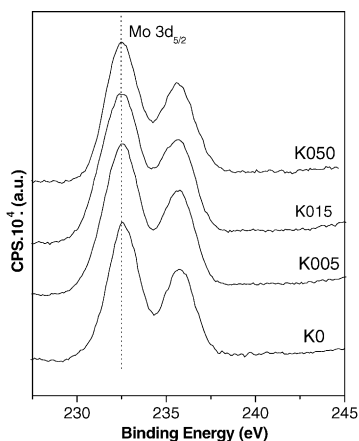


Fig. 4. Mo 3d_{5/2} XP spectra of catalysts.

Table 2
XPS results of K-MoO_x/ZrO₂ catalysts

Catalyst	Binding energy (eV)			Surface atomic ratio ^a			Bulk atomic ratio ^b	
	K 2p _{3/2}	Zr 3d _{5/2}	Mo 3d _{5/2}	K/Zr	K/Mo	Mo/Zr	K/Zr	Mo/Zr
K0	–	182.2	232.5	–	–	0.25	–	0.11
K005	293.0	182.2	232.5	0.01	0.05	0.28	0.006	0.11
K015	293.2	182.2	232.5	0.03	0.12	0.24	0.016	0.11
K050	293.2	182.2	232.6	0.09	0.45	0.21	0.056	0.11

^a Experimental surface ratio calculated by XPS data.

^b Preparation composition of the catalysts.

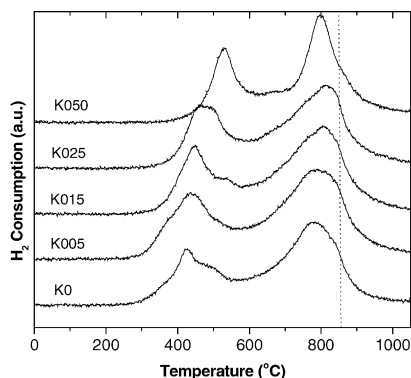


Fig. 5. TPR profiles of K-MoO_x/ZrO₂.

shown in Table 2. The binding energies of Mo 3d_{5/2} vary in a narrow range between 232.5 and 232.6 eV. This corresponds to Mo⁶⁺ in an environment of oxide anions [26]. Both K and Mo surface atomic ratios are higher than the theoretical bulk atomic ratios indicating the migration of K and Mo to the surface.

TPR results of the catalysts up to 850 °C are given in Fig. 5. The first peak in the K-free sample has a maximum at 444 °C, which shifts to 522 °C at the catalyst with the highest K content. This peak can be ascribed to the reduction of Mo(VI) to Mo(IV) and the second peak can be attributed to the reduction of Mo(IV) to lower valence states [27]. The peak maxima are given in Table 3.

3.2. Catalytic measurements

The propane conversion and product selectivity results of the catalytic activity experiments at 450 and 500 °C are given in Table 4. As expected, propylene as well as carbon monoxide and carbon dioxide were main products. In addition,

Table 3
TPR peak maxima of K-MoO_x/ZrO₂ catalysts

Catalyst	Temperature (°C)	
	1st peak	2nd peak
K0	444	801
K005	457	809
K015	469	831
K025	489	820
K050	522	800

Table 4
ODH of propane catalytic measurement results over K-MoO_x/ZrO₂ catalysts

Catalyst	T (°C)	Conversion (%)	Selectivity (%)			
			C ₃ H ₈	C ₃ H ₆	CO	CO ₂
K0	450	18.3	21.2	50.1	28.6	0.1
	500	28.3	18.6	59.8	21.2	0.2
K005	450	11.3	42.8	41.1	16.0	0.1
	500	31.2	25.1	52.3	22.4	0.2
K015	450	7.1	49.1	20.5	30.4	0.0
	500	16.7	44.9	28.8	26.2	0.1
K025	450	2.6	51.7	32.3	16.0	0.0
	500	5.4	55.4	33.1	11.5	0.0
K050	450	3.6	42.9	25.9	31.2	0.0
	500	5.3	43.2	32.5	23.8	0.5

ethylene and trace amounts of methane and ethane were also detected.

K addition affected both propane conversion and propylene selectivity. The effect of K/Mo ratio on conversion, and propylene selectivity at 530 °C are given in Fig. 6. Propane conversion at 530 °C increased for K005 and then decreased below to K-free catalyst level for K015. The propylene selectivity of 18.8% for K-free catalyst increased to 52.1% for K025 and then decreased for K050. The effect of reaction temperature on propylene selectivity is shown in Fig. 7. Propylene selectivity decreased with temperature on both K-free and those with low K-loaded catalysts, namely K005 and K015, but the selectivity increased at higher potassium loadings. The specific activity and propylene productivity results at 530 °C are given in Table 5. The propylene productivity

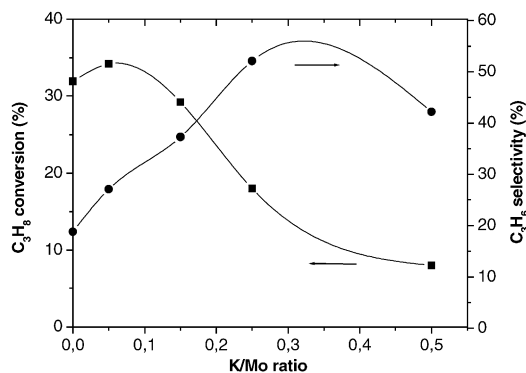


Fig. 6. The effect of K addition on propane conversion and selectivity at 530 °C.

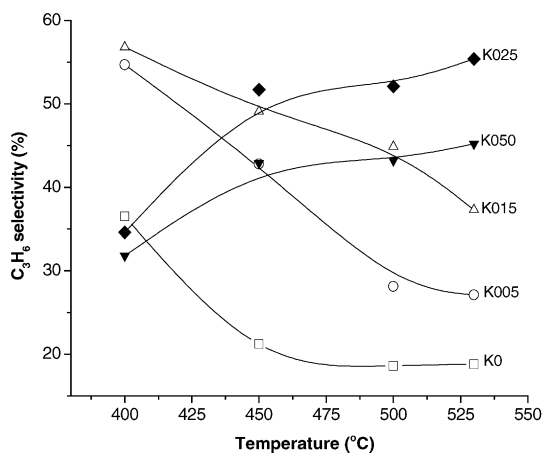


Fig. 7. The effect of reaction temperature on propylene selectivity.

Table 5
Specific activity and propylene productivity results of K-MoO_x/ZrO₂ catalysts

Catalyst	Specific activity $\mu\text{mol C}_3\text{H}_8 \text{ m}^{-2} \text{ s}^{-1} \times 10^{-5}$	Propylene productivity $\text{kg C}_3\text{H}_6/\text{kgcat h}$
K0	2.02	0.044
K005	2.45	0.070
K015	1.73	0.082
K025	1.14	0.061
K050	0.61	0.027

values of K-loaded catalysts except K050 are higher than that of K-free catalyst. Fig. 8 shows the propylene yields of the catalysts at 530 °C. The propylene yield of 6.1% for K-free sample increased to 10.9% upon 15% K addition. The conversion–selectivity plots of K-free and K015 catalysts are shown in Fig. 9. The propylene selectivity of both catalysts decreased with the increase in conversion and the presence of 15% potassium enhanced the selectivity in comparison to those of K-free catalyst.

4. Discussion

In this work, we investigated the ODH of propane over K loaded MoO_x/ZrO₂ catalysts prepared by the sol–gel method.

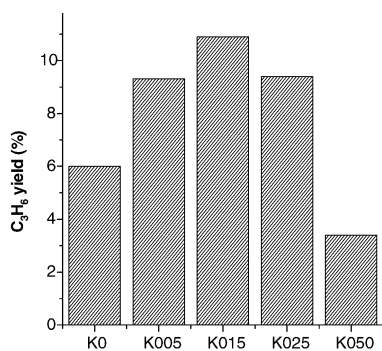


Fig. 8. The effect of K addition on propylene yield at 530 °C.

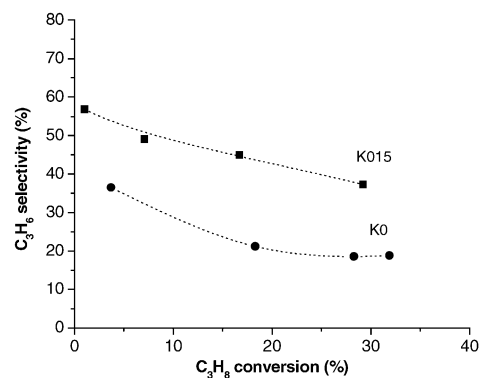


Fig. 9. The conversion and selectivity plot of K0 and K015 catalysts.

Alkali addition by impregnation generally reduces surface area by blocking the pores. In the case of sol–gel method employed in this work, this addition was well tolerated and the surface area even increased at a certain level of potassium loading. Furthermore, alkali or acid addition regulates the hydrolysis and condensation reactions in sol–gel method during gelation and affects the surface area and pore volumes [28,29]. This provided the steady increase in pore volumes with the increases in K loading up to a certain level.

It was observed from the XRD and Raman spectroscopy measurements that molybdenum oxides form Zr(MoO₄)₂ to a large extent in the absence of potassium. Although the calcination was carried out at 540 °C, no peak ascribed to crystalline monoclinic zirconia was observed in XRD and Raman spectra due to the stabilization effect of MoO_x units distributed in tetragonal phase of zirconia [19]. As K content of the catalyst increased, it was observed that the intensity of the peak at 745 cm⁻¹ due to Zr(MoO₄)₂ phase decreased and finally disappeared, but the intensity of tetragonal zirconia peaks (312, 456, and 648 cm⁻¹) increased. K probably either attacks Mo–O–Zr bonds or reduces the interface between MoO_x and zirconia, and as a result suppresses the formation of Zr(MoO₄)₂. In addition, intensities of three-dimensional molybdenum oxide aggregates and two-dimensional polymolybdate in Raman spectra increased with potassium loading. It is known that two-dimensional polymolybdate domains can be formed by condensation of isolated molybdenum oxide species or by spreading of three-dimensional molybdenum oxides on the surface during calcination [30,31]. Since the Raman measurement of the K-free catalyst showed the absence of isolated species, spreading mechanism of three-dimensional molybdenum oxides has probably occurred in these catalysts. Furthermore, the K and Mo migration occurred during calcination because surface atomic ratios of both elements are higher than theoretical values as indicated by XPS. The shift of Raman peaks of lower potassium loaded catalysts from 970 to 960 cm⁻¹ with slight broadening for K050 catalyst may be attributed to K incorporation to molybdenum oxide, as similarly reported by Bian et al. [32]. The increase in reduction peak of Mo(VI) in

TPR curves from 444 to 522 °C with K loading confirms the effect of K on the reduction properties of molybdenum oxide units.

Catalytic reaction data showed that K-free catalyst has higher activity in propane oxidative dehydrogenation, but lower selectivity to propylene. Chen et al. [13] reported that $Zr(MoO_4)_2$ phase is active, but it does not have higher propylene selectivity in ODH of propane than that of molybdenum oxides. It is also known that potassium incorporation to molybdenum oxide units contributes to the propylene desorption from the catalyst surface by decreasing the acidity of catalytically active sites as reported by Watson and Ozkan [16]. Since propylene is strongly adsorbed by acidic sites, it is easily converted to combustion products due to its weaker allylic C–H bonds [3]. These findings explain the improvement in propylene selectivity from 18.8 to 52.1% by potassium loading at 530 °C in this study. It was also observed that K incorporation did not drastically decrease propane conversion up to K015. For this reason, K loading increased propylene yield of the catalysts such that 6.1% over K-free catalyst was improved up to 10.9% upon 15% K loading. In addition, propylene selectivity of K-free catalyst decreased with reaction temperature (Fig. 7). But, potassium loading led to an increase in propylene selectivity at higher temperatures. Why propylene selectivity was improved by K loading even though propane conversion increase can be attributed to the positive effect of alkali incorporation on the selectivity. It is known that adsorbed oxygen species lead to the formation of CO_x more than lattice oxygen does. In addition, potassium suppresses the surface potential favoring oxygen insertion from surface to the lattice vacancies produced by the reduction of molybdenum oxide [33]. As a result, oxygen insertion from surface to the lattice vacancies as well as propylene desorption from the surface could be easier in the presence of alkali promoter. In both cases, propylene selectivity increased at higher reaction temperatures.

5. Conclusion

Potassium addition affected the structures of both molybdenum oxide and zirconia support, and prevented the formation of crystalline $Zr(MoO_4)_2$ by suppressing the interaction of molybdenum oxide with zirconia. It also contributed to the formation of three-dimensional molybdenum oxide aggregates and two-dimensional polymolybdate units. Propylene selectivity and yield increased with certain amount of potassium loading. With the exception of the catalyst with 0.5 molar ratio of K to Mo, all catalysts gave higher propylene yield than that of K-free catalyst.

Acknowledgement

This work was supported by the Research Fund of Istanbul University, Project No: 1448/05052000 and partly by DAAD (German Academic Exchange Service), Project No: 309.104401.009.

References

- [1] T. Blasco, J.M. Lopez Nieto, *Appl. Catal. A* 157 (1997) 142.
- [2] M.M. Bettahar, G. Kostentin, L. Savary, L.C. Lavalley, *Appl. Catal. A* 145 (1996) 1.
- [3] H.H. Kung, *Adv. Catal.* 40 (1994) 1.
- [4] C. Mazzochia, E. Tempesti, U.S. Patent No: 5086032, 1992.
- [5] B. Grzybowska, P. Mekss, R. Grabowski, K. Wcislo, Y. Barbaux, L. Gengembre, *New Developments in Selective Oxidation II*, 151, Elsevier, 1994.
- [6] Y.S. Yoon, N. Fujikawa, W. Ueda, Y. Moro-oka, K.W. Lee, *Catal. Today* (1995) 327.
- [7] L.E. Cadus, M.C. Abello, M.F. Gomez, J.B. Rivarola, *Ind. Eng. Chem. Res.* 35 (1996) 14.
- [8] O. Lezla, E. Bordes, P. Courtine, G. Hecquet, *J. Catal.* 170 (1997) 346.
- [9] D.L. Stern, R.K. Graselli, *J. Catal.* 167 (1997) 560.
- [10] F.C. Meunier, A. Yasmeen, J.R.H. Ross, *Catal. Today* 37 (1997) 33.
- [11] K. Chen, S. Xie, A.T. Bell, E. Iglesia, *J. Catal.* 198 (2001) 232.
- [12] J.E. Miller, N.B. Jackson, L. Evans, A.G. Sault, M.M. Gonzales, *Catal. Lett.* 58 (1999) 147.
- [13] K. Chen, S. Xie, E. Iglesia, A.T. Bell, *J. Catal.* 189 (2000) 421.
- [14] L.J. Duhamel, A. Ponchel, Y. Barbaux, *J. Chim. Phys.* 94 (1997) 1975.
- [15] K. Chen, S. Xie, A.T. Bell, E. Iglesia, *J. Catal.* 195 (2000) 244.
- [16] R.B. Watson, U.S. Ozkan, *J. Catal.* 191 (2000) 12.
- [17] D.A. Ward, E.I. Ko, *Ind. Eng. Chem. Res.* 34 (1995) 421.
- [18] M.A. Cauqui, J.M. Rodriguez, *J. Non-Cryst. Solids* 147 (1992) 723.
- [19] P. Afanasiev, M.A. Thiollier, M. Breyse, J.B. Dubois, *Top. Catal.* 8 (1999) 147.
- [20] J. Miciukiewicz, H. Knözinger, *Appl. Catal. A* 122 (1995) 151.
- [21] B. Zhao, X. Wang, H. Ma, Y. Tang, *J. Mol. Catal. A* 108 (1996) 167.
- [22] B. Zhao, X. Xu, H. Ma, D. Sun, J. Gao, *Catal. Lett.* 45 (1997) 237.
- [23] P.D.L. Mercera, J.G. Van Ommen, E.B.M. Doesburg, A.J. Burggraaf, *Appl. Catal.* 57 (1990) 127.
- [24] S. Xie, K. Chen, A.T. Bell, E. Iglesia, *J. Phys. Chem. B* 104 (2000) 10059.
- [25] I.E. Wach, *Catal. Today* 27 (1996) 437.
- [26] M.C. Abello, M.F. Gomez, M. Casella, O.A. Ferretti, M.A. Bañares, J.L.G. Fierro, *Appl. Catal. A: Gen.* 251 (2003) 435.
- [27] P. Arnoldy, J.C.M. Jonge, J.A. Moulijn, *J. Phys. Chem.* 89 (1985) 4517.
- [28] L.L. Hench, J.K. West, *Chem. Rev.* 90 (1990) 33.
- [29] C.J. Brinker, D.W. Scherer, *Sol-Gel Science*, Academic Press, New York, 1990.
- [30] P.A. Spevack, S. McIntyre, *J. Phys. Chem.* 97 (1993) 11020.
- [31] C.C. Williams, J.G. Ekerdt, *J. Phys. Chem.* 95 (1991) 8791.
- [32] G. Bian, L. Fan, Y. Fu, K. Fujimoto, *Appl. Catal. A* 170 (1998) 255.
- [33] B.G. Swierkosz, *Top. Catal.* 11/12 (2000) 23.